Hindawi
Wireless Communications and Mobile Computing
Volume 2021, Article ID 5539572, 9 pages
https://doi.org/10.1155/2021/5539572

Research Article

Robust Secure Energy Efficiency Optimization in the MIMO Wiretap Channel with Energy Harvesting

Wenfeng Ma, Cong Wang, Hui Tian, Xun Cao, and Yuanxiang Yao

College of Field Engineering, Army Engineering University, Nanjing, China

Correspondence should be addressed to Hui Tian; jaytianhui@foxmail.com

Received 7 January 2021; Revised 19 August 2021; Accepted 23 August 2021; Published 30 September 2021

Academic Editor: Mohammed El-Hajjar

This work considers a secure multiple-input multiple-output (MIMO) channel where the energy receiver (ER) is a potential eavesdropper (Eve). Specifically, we aim to maximize the secrecy energy efficiency (SEE) via jointly designing the transmit precoding matrix and the artificial noise (AN) covariance at the base station (BS), as well as the power splitting (PS) ratio at the desired receiver (DR), subject to the constraints of the transmit power budget and harvested energy threshold. To handle the formulated highly nonconvex fractional problem, we apply the successive convex approximation (SCA) method to transform the objective and constraint into a tractable form. Then, a penalty-based iterative algorithm is proposed. Finally, simulation results validate the performance of the proposed design.

1. Introduction

Simultaneous wireless information and power transfer (SWIPT) and energy efficiency (EE) transmission are considered two prominent approaches to the ever increasing demand for energy in the context of next-generation communication [1]. More specifically, in SWIPT-based communications, the receivers are able to salvage electromagnetic energy from radiofrequency (RF) signals. On the other hand, energy-efficient communication is aimed at achieving a certain rate-energy balance by maximizing the EE, defined as the number of delivered bits per unit energy [2].

Traditionally, SWIPT and EE are often independently investigated. Recently, there is growing interest in combining these two concepts together to maximize the EE in the SWIPT system in [3]. Several authors characterized the capacity and energy tradeoffs for SWIPT under different system setups, such as the multiple-input multiple-output (MIMO) channel in [4] and the amplify-and-forward (AF) relay networks [5].

It is a fundamental requirement for the next-generation wireless communication systems to provide secure communication. As a complement to traditional cryptographic encryption, a large amount of literature has been devoted to the physical-layer security (PLS), especially in multiantenna systems [6]. Taking full advantage of the spatial degrees of freedom (DoF) offered by multiple transmit antennas, the transmitter could enhance the overall security by the means of transmit beamforming (BF) and artificial noise (AN) [7]. The effectiveness of transmit BF and AN has also been verified in the secure SWIPT system [8].

Since the goal of secrecy throughput maximization may conflict with the aim of harvested energy maximization, secure EE (SEE) can be considered a performance metric for studying the tradeoff between these two goals. Specifically, for the SEE design, in [9], the authors investigated an artificial noise-aided energy efficiency optimization in the MIMO channel with SWIPT, while in [10], the authors investigated the secure and energy-efficient BF design for multiuser downlink multiple-input single-output (MISO) channel with SWIPT.

From a more practical view, the channel state information (CSI) of the eavesdropper (Eve) may not be perfect obtained by the transmitter due to the existence of channel estimation, quantization, or feedback errors; thus, robust secrecy design has been widely investigated. Specifically, in [11, 12], the authors studied the robust secrecy design in the MISO channel, based on the probabilistic constrained robust model and the worst case robust model, respectively, while in [13], the authors investigated the robust harvested energy efficiency optimization for secure MIMO SWIPT systems. In [14], the authors investigated the robust BF designs for secrecy MIMO SWIPT systems, while in [15, 16], the authors investigated the outage constrained robust secrecy rate maximization and secrecy energy efficiency maximization design with SWIPT, respectively. The above works were focused on the linear RF energy harvesting (EH) model. Furthermore, by considering a practical nonlinear EH model, in [17], the authors studied the robust BF design in a nonorthogonal multiple access (NOMA) network relying on SWIPT. In [18], the authors studied the computation efficiency maximization in wireless-powered mobile edge computing networks. Moreover, in [19], the authors investigated the AN-aided secure cognitive BF for cooperative MISO-NOMA using SWIPT, while in [20], the authors studied the EE optimization in secure MISO SWIPT systems with a nonlinear EH model. However, these works mainly focus on the MISO channel, and the SEE in the MIMO SWIPT channel has not been investigated yet.

Motivated by these observations, in this work, we focus on the robust SEE design for a SWIPT-based MIMO wiretap channel, where the desired receiver (DR) employs the power splitting (PS) scheme to facilitate the SWIPT and AN is emitted by the transmitter to improve the security. Specifically, we aim to maximize the ratio of the secrecy rate with the total power consumption, by jointly designing the precoding matrix, AN covariance, and the PS ratios. Different from the commonly used Dinkelbach method, we apply the successive convex approximation (SCA) method to transform the constraints into tractable forms, where the fractional objective is turned into exponential functions. Then, to reduce the performance loss introduced by the rank relaxation, a penalty-based iterative algorithm is proposed. Finally, numerical results indicate the performance of the proposed design and provide some meaningful insights.

Our contributions are summarized as follows:

(1) To the best of our knowledge, this is the first work to study the SEE optimization in a MIMO SWIPT network. The formulated problem is nonconvex due to the nonconvex objective, the nonconvex constraints, the coupled variables, and the infinite constraints arising from the CSI uncertainty

(2) Different from the Dinkelbach algorithm, we do not transform the fractional programming into a subtractive form. However, we directly handle the fractional objective, which is no need of the one-dimensional search procedure, thus reducing the computational complexity. Specifically, a SCA method is utilized to decompose and reformulate the original nonconvex problem, while the CSI error is tackled by the S-procedure. Then, a penalty-based iterative algorithm is proposed to optimize the BF, the AN covariance, and the PS ratio

(3) The computational complexity of the proposed algorithm is analyzed, which suggests that the proposed algorithm has lower complexity. Simulation results show that the proposed design achieves better SEE than other benchmarks. Besides, some meaningful insights are given by the results: (1) AN can improve the SEE in the wiretap channel evidently, (2) the dynamic PS scheme can attain higher SEE than the fixed PS scheme, and (3) the linear EH model is more beneficial to improve the SEE than the nonlinear EH model

The rest of this work is organized as follows. The system model and problem statement are given in Section 2. Section 3 investigates the joint precoding, AN, and PS design, where a SCA-based algorithm is proposed. Simulation results are provided in Section 4. Section 5 concludes this work.

1.1. Notations. Throughout this work, boldface lowercase and uppercase letters denote vectors and matrices, respectively. The conjugate, transpose, conjugate transpose, and trace of matrix A are denoted as $\mathbf{A}^{\dagger}$, $\mathbf{A}^{T}$, $\mathbf{A}^{H}$, and $\mathrm{Tr}(\mathbf{A})$, respectively. $\boldsymbol{a} = \mathrm{vec}(\mathbf{A})$ denotes stacking the columns of matrix $\mathbf{A}$ into a vector a. $\mathbf{A} \succcurlyeq 0$ indicates that $\mathbf{A}$ is a positive semidefinite matrix. $\|\boldsymbol{a}\|$ denotes the Euclidean norm of vector a. e denotes the element-wise product. $\mathbf{I}$ is an identity matrix with proper dimension. $\mathscr{CN}(\mathbf{0}, \mathbf{I})$ denotes a circularly symmetric complex Gaussian random vector with mean $\mathbf{0}$ and covariance $\boldsymbol{I}$. $[x]^{+}$ indicates $\max(0, x)$.

2. System Model and Problem Statement

2.1. System Model. Let us consider a MIMO downlink system as shown in Figure 1, which consists of one transmitter, one DR, and M energy receivers (ERs). In the network, the DR employs a PS scheme to extract information and power simultaneously while the ER is potential Eve. It is assumed that the transmitter, the DR, and each ER are equipped with N_T, N_D, and N_E antennas, respectively. The channel coefficients between the transmitter and the DR, as well as the m-th ER, $m \in M = \{1, \cdots, M\}$, are denoted as $\boldsymbol{H} \in \mathbb{C}^{N_T \times N_D}$ and $\mathbf{G}_m \in \mathbb{C}^{N_T \times N_E}$, respectively.

In this work, we assume that only imperfect ERs' CSI can be attained. Similar to [13], the imperfect CSI can be modeled as

$$\mathscr{G}_m = \left\{ \mathbf{G}_m \middle| \mathbf{G}_m = \bar{\mathbf{G}}_m + \Delta\mathbf{G}_m, \|\Delta\mathbf{G}_m\|_F \le \varepsilon_m \right\}, \quad (1)$$

where $\bar{G}_m$ denotes the estimate of the true G_m, ΔG_m denotes their respective error, and ε_m represents the respective size of the bounded error region.

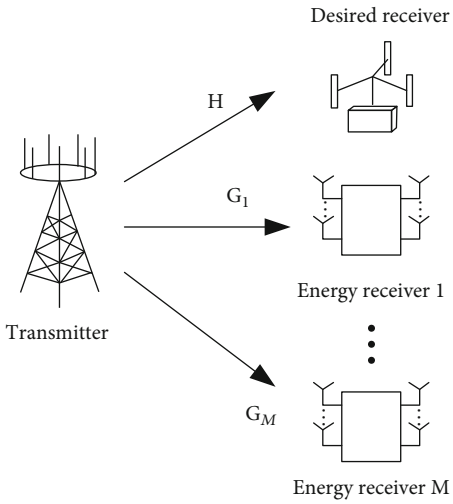

Figure 1: The secure MIMO SWIPT system.

The information bearing the signal vector $s \in \mathbb{C}^{d\times 1}$ ($d \le N_T$) is precoded by the precoding matrix $W \in \mathbb{C}^{N_T\times d}$, and AN is used to help energy transfer and improve security. Thus, the transmit signal vector $x \in \mathbb{C}^{N_T\times 1}$ can be expressed as

$$x = \mathbf{W}s + v, \tag{2}$$

where $v \in \mathbb{C}^{N_T\times 1}$ is the AN vector with $v \sim \mathscr{CN}(0, Z)$. Without loss of generality (W.l.o.g.), we assume that $\mathbb{E}[ss^H] = \mathbf{I}$.

The total transmit power is

$$P_{\text{tot}}(\mathbf{W}, \mathbf{Z}) = \mu \text{Tr}\left(\mathbf{W}\mathbf{W}^H + \mathbf{Z}\right) + P_c, \tag{3}$$

where μ is the transmitter power amplifier efficiencies, respectively. In addition, P_c is the total circuit power consumption for the network.

Then, the received signals at the DR and the m-th ER can be expressed as

$$\boldsymbol{y}_D = \mathbf{H}^H\mathbf{W}s + \mathbf{H}^H\mathbf{z} + \mathbf{n}_D, \tag{4a}$$

$$\boldsymbol{y}_{E,m} = \mathbf{G}_m^H\mathbf{W}\mathbf{s} + \mathbf{G}_m^H\mathbf{z} + \mathbf{n}_{E,m}, \tag{4b}$$

where $\mathbf{n}_D \in \mathbb{C}^{N_D\times 1}$ and $\mathbf{n}_{E,m} \in \mathbb{C}^{N_E\times 1}$ are the noise vectors at the DR and the m-th ER with $\mathbf{n}_D \sim \mathscr{CN}(\mathbf{0}, \sigma_D^2\mathbf{I})$ and $\mathbf{n}_{E,m} \sim \mathscr{CN}(\mathbf{0}, \sigma_{E,m}^2\mathbf{I})$, respectively.

The received signals at the DR are divided into two streams. One is used to information decoding (ID), and the other is for EH. Specifically, by denoting ρ as the PS ratio at the DR, the signal received for ID and EH at the DR can be expressed as

$$\boldsymbol{y}_{D,I} = \sqrt{\rho}\left(\mathbf{H}^H\mathbf{W}s + \mathbf{H}^H\mathbf{z} + \mathbf{n}_D\right) + \mathbf{n}_P, \tag{5a}$$

$$y_{D,E} = \sqrt{1-\rho}\left(\mathbf{H}^H\mathbf{W}s + \mathbf{H}^H\mathbf{z} + \mathbf{n}_D\right), \tag{5b}$$

where $\mathbf{n}_P \in \mathbb{C}^{N_D\times 1}$ is the additional processing noise at the DR with $n_P \sim \mathscr{CN}(0, \sigma_P^2\mathbf{I})$. It should be noted that, when the harvested power is relatively small, the nonlinear EH model can be approximated as a linear EH model [20]. Thus, in this work, we adapt the linear EH model due to the simplicity. Furthermore, in the simulation part, we will compare the SEE performance in linear and nonlinear EH models, respectively.

Accordingly, the achievable secrecy rate can be expressed as

$$R_s(\rho, \mathbf{W}, \mathbf{Z}) = C_D - \max_{\forall m\in M} C_{E,m}, \tag{6}$$

where C_D and $C_{E,m}$ denote the mutual information at the DR and the m-th ER, respectively, and are given by

$$C_D = \ln\left|\mathbf{I} + \frac{\rho\mathbf{H}^H\mathbf{W}\mathbf{W}^H\mathbf{H}}{\rho\sigma_D^2\mathbf{I} + \rho\mathbf{H}^H\mathbf{Z}\mathbf{H} + \sigma_P^2\mathbf{I}}\right|, \tag{7a}$$

$$C_{E,m} = \ln\left|\mathbf{I} + \frac{G_m^H\mathbf{W}\mathbf{W}^H\mathbf{G}_m}{\sigma_{E,m}^2\mathbf{I} + G_m^H\mathbf{Z}\mathbf{G}_m}\right|. \tag{7b}$$

On the other hand, the received RF power at the DR and the m-th ER can be expressed as

$$E_D = \alpha(1-\rho)\text{Tr}\left(\mathbf{H}^H\left(\mathbf{W}\mathbf{W}^H + \mathbf{Z}\right)\mathbf{H}\right), \tag{8a}$$

$$E_{E,m} = \eta_m\text{Tr}\left(\mathbf{G}_m^H\left(\mathbf{W}\mathbf{W}^H + \mathbf{Z}\right)\mathbf{G}_m + \sigma_{E,m}^2\mathbf{I}\right), \tag{8b}$$

where α and η_m denote the energy transform efficiency at the DR and the m-th ER, respectively.

Therefore, the SEE for the MIMO network is defined as

$$\text{SEE}(\rho, \mathbf{W}, \mathbf{Z}) = \frac{R_s(\rho, \mathbf{W}, \mathbf{Z})}{P_{\text{tot}}(\mathbf{W}, \mathbf{Z})}\,[\text{bit/Joule}]. \tag{9}$$

2.2. Problem Statement. In this work, we aim to maximize the SEE via jointly designing the transmit precoding matrix and the AN covariance at the transmitter, as well as the PS ratio at the DR, subject to the constraints of the transmit power budget and harvested energy threshold. Specifically, the SEE maximization problem subject to the worst case secrecy rate and minimum EH threshold constraint can be formulated as

$$\text{P1}: \max_{\rho,\mathbf{W},\mathbf{Z}} \text{SEE}(\rho, \mathbf{W}, \mathbf{Z}), \tag{10a}$$

$$\text{s.t.} E_D(\rho, \mathbf{W}, \mathbf{Z}) \ge E_{D,th}, \tag{10b}$$

$$E_m(\mathbf{W}, \mathbf{Z}) \ge E_{m,th}, \tag{10c}$$

$$P_{\text{tot}}(\mathbf{W}, \mathbf{Z}) \le P_s, \tag{10d}$$

$$R_s(\rho, \mathbf{W}, \mathbf{Z}) \ge R_{th}, \tag{10e}$$

$$\mathbf{Z} \succcurlyeq \mathbf{0}, 0 \le \rho \le 1, \tag{10f}$$

where $E_{R,th}$ and $E_{m,th}$ are the minimum harvested energy threshold at the DR and the m-th ER, respectively. In addition, R_{th} is the minimum secrecy rate and P_s is the maximum transmit power.

In fact, there exists another commonly used robust design, e.g., the probabilistic constrained robust design [21], where the authors studied the robust trajectory and transmit power optimization for secure unmanned aerial vehicle- (UAV-) enabled networks and proposed a fair comparison between the performance of the worst case design and the outage case design by setting the radii of the bounded uncertainty regions to a certain value, which is given by $\varepsilon_m = \varpi_m \sqrt{F^{-1}_{2N_T N_E+2}(1-\varphi)}$, where $F^{-1}_{2N_T N_E+2}(\cdot)$ denotes the inverse cumulative distribution function of a chi-square random variable with $2N_T N_E + 2$ degrees of freedom, φ denotes the outage probability, and ϖ_m is the region for the probabilistic CSI uncertainty; e.g., we assume that $\mathrm{vec}(\Delta G_m) \sim \mathscr{CN}(0, \varpi_m^2 I)$.

Thus, in this work, we mainly focus on the bounded CSI uncertainty, since the proposed method can be extended to the probabilistic constrained case.

3. A SCA-Based Method for the SEE Design

P1 is a typical fractional programming, different from the commonly used Dinkelbach algorithm in [22]; we will propose an effective method to handle this obstacle.

Firstly, we need to turn $R_s(\rho, \mathbf{W}, \mathbf{Z})$ into a solvable reformation. Via denoting $\mathbf{Q} = \mathbf{W}\mathbf{W}^H$ and $t = 1/\rho$, we obtain the following problem:

$$\mathrm{P2}: \max_{\mathbf{Q},\mathbf{Z},t,\gamma_1,\gamma_2} \frac{\gamma_1 - \gamma_2}{\mu \mathrm{Tr}(\mathbf{Q}+\mathbf{Z}) + P_c}, \tag{11a}$$

$$\mathrm{s.t.} \gamma_R \geq \gamma_1, \tag{11b}$$

$$\gamma_m \leq \gamma_2, \forall \mathbf{G}_m \in \mathbf{G}_m, \tag{11c}$$

$$\alpha\left(1 - \frac{1}{t}\right)\mathrm{Tr}\left(\mathbf{H}^H(\mathbf{Q}+\mathbf{Z})\mathbf{H} + \sigma_D^2\mathbf{I}\right) \geq E_{R,th}, \tag{11d}$$

$$\eta_m \mathrm{Tr}\left(\mathbf{G}_m^H(\mathbf{Q}+\mathbf{Z})\mathbf{G}_m + \sigma_{E,m}^2\mathbf{I}\right) \geq E_{m,th}, \forall \mathbf{G}_m \in \mathscr{G}_m, \tag{11e}$$

$$\mu \mathrm{Tr}(\mathbf{Q}+\mathbf{Z}) + P_c \leq P_s, \tag{11f}$$

$$\mathbf{Q} \succcurlyeq \mathbf{0}, \mathbf{Z} \succcurlyeq \mathbf{0}, t \geq 1, \tag{11g}$$

$$\gamma_1 - \gamma_2 \geq R_{th}, \tag{11h}$$

where γ_R and γ_k are given as

$$\gamma_R = \ln\left|\mathbf{H}^H(\mathbf{Q}+\mathbf{Z})\mathbf{H} + \sigma_D^2\mathbf{I} + t\sigma_P^2\mathbf{I}\right| - \ln\left|\mathbf{H}^H\mathbf{Z}\mathbf{H} + \sigma_D^2\mathbf{I} + t\sigma_P^2\mathbf{I}\right|, \tag{12a}$$

$$\gamma_m = \ln\left|\mathbf{G}_m^H(\mathbf{Q}+\mathbf{Z})\mathbf{G}_m + \sigma_{E,m}^2\mathbf{I}\right| - \ln\left|\mathbf{G}_m^H\mathbf{Z}\mathbf{G}_m + \sigma_{E,m}^2\mathbf{I}\right|, \forall \mathbf{G}_m \in \mathscr{G}_m, \tag{12b}$$

and γ_1 and γ_2 are the auxiliary variables.

The main difficulty of (11) is that (11b) and (11c) are the difference of convex functions; thus, P2 is still nonconvex. To overcome this difficulty, we will approximate these terms via the first-order Taylor expansion at a fixed point.

Specifically, around given point $\{\tilde{\mathbf{Q}}, \tilde{\mathbf{Z}}, \tilde{t}\}$, we have

$$\tilde{\gamma}_R = \ln\left|\mathbf{H}^H(\mathbf{Q}+\mathbf{Z})\mathbf{H} + \sigma_D^2\mathbf{I} + t\sigma_P^2\mathbf{I}\right| - \ln|\mathbf{A}| - \mathrm{Tr}\left(\mathbf{A}^{-1}\mathbf{H}^H\left(\mathbf{Z}-\tilde{\mathbf{Z}}\right)\mathbf{H}\right) - \mathrm{Tr}\left(\mathbf{A}^{-1}\left(t-\tilde{t}\right)\sigma_P^2\mathbf{I}\right), \tag{13a}$$

$$\tilde{\gamma}_m = \ln|\mathbf{B}_m| + \mathrm{Tr}\left(\mathbf{B}_m^{-1}\mathbf{G}_m^H\left(\mathbf{Q}-\tilde{\mathbf{Q}}+\mathbf{Z}-\tilde{\mathbf{Z}}\right)\mathbf{G}_m\right) - \ln\left|\mathbf{G}_m^H\mathbf{Z}\mathbf{G}_m + \sigma_{E,m}^2\mathbf{I}\right|, \tag{13b}$$

where $\mathbf{A} = \mathbf{H}^H\tilde{\mathbf{Z}}\mathbf{H} + \sigma_D^2\mathbf{I} + \tilde{t}\sigma_P^2\mathbf{I}$ and $\mathbf{B}_m = \bar{\mathbf{G}}_m{}^H(\tilde{\mathbf{Q}}+\tilde{\mathbf{Z}})\bar{\mathbf{G}}_m + \sigma_{E,m}^2\mathbf{I}$, respectively.

Thus, we have the following approximated problem:

$$\mathrm{P3}: \max_{\mathbf{Q},\mathbf{Z},t,\gamma_1,\gamma_2} \frac{\gamma_1 - \gamma_2}{\mu \mathrm{Tr}(\mathbf{Q}+\mathbf{Z}) + P_c}, \tag{14a}$$

$$\mathrm{s.t.}(11\mathrm{d}) - (11\mathrm{h}), \bar{\gamma}_R \geq \gamma_1, \bar{\gamma}_m \leq \gamma_2. \tag{14b}$$

Nextly, we will focus on the CSI uncertainties in $\mathbf{G}_m$. By introducing slack variables $\{\zeta_m, \theta_m\}$, the constraint $\bar{\gamma}_m \leq \gamma_2$ can be rewritten as

$$\ln\left|\sigma_{E,m}^2\mathbf{I} + \mathbf{G}_m^H\mathbf{Z}\mathbf{G}_m\right| \geq \ln\zeta_m, \tag{15a}$$

$$\ln|\mathbf{B}_m| + \mathrm{Tr}\left(\mathbf{B}_m^{-1}\mathbf{G}_m^H\left(\mathbf{Q}-\tilde{\mathbf{Q}}+\mathbf{Z}-\tilde{\mathbf{Z}}\right)\mathbf{G}_m\right) \leq \theta_m, \tag{15b}$$

$$\theta_m \leq \ln\zeta_m + \gamma_2. \tag{15c}$$

To transform (15a) and (15b) into deterministic reformations, we introduce the following lemma.

Lemma 1 [13]. *For any positive semidefinite matrix* $\mathbf{A}$*, the inequality holds* $|\mathbf{I}+\mathbf{A}| \geq 1 + Tr(\mathbf{A})$ *and the equality holds if and only if* $\mathrm{rank}(\mathbf{A}) \leq 1$.

According to Lemma 1, we obtain the following relationship:

$$\begin{aligned}(15\mathrm{a}) &\Longleftrightarrow \sigma_{E,m}^{2N_E}\left|\mathbf{I} + \sigma_{E,m}^{-2}\mathbf{G}_m^H\mathbf{Z}\mathbf{G}_m\right| \geq \zeta_m \\ &\Longleftarrow \mathrm{Tr}\left(\mathbf{G}_m^H\mathbf{Z}\mathbf{G}_m\right) \geq \sigma_{E,m}^{2(1-N_E)}\zeta_m - \sigma_{E,m}^2.\end{aligned} \tag{16}$$

Then, we vectorized the equation $\mathbf{G}_m = \bar{\mathbf{G}}_m + \Delta\mathbf{G}_m$; e.g., we denote $g_m = \mathrm{vec}(\mathbf{G}_m)$, $\bar{\mathbf{g}}_m = \mathrm{vec}(\bar{\mathbf{G}}_m)$, $\Delta\mathbf{g}_m = \mathrm{vec}(\Delta\mathbf{G}_m)$; it is easy to know that $\|\Delta\mathbf{G}_m\|_F \leq \varepsilon_m \Longrightarrow \|\Delta\mathbf{g}_m\|_2 \leq \varepsilon_m$.

By using the identity $\mathrm{Tr}(AB^HCD) = \mathrm{vec}(B)^H(A^T \otimes C)\,\mathrm{vec}(D)$, we transform (16) to

$$\begin{cases} \Delta g_m^H \Delta g_m - \delta_m^2 \le 0, \\ -\bar{g}_m^H (I \otimes Z)\bar{g}_m - 2\Re\left\{\bar{g}_m^H (I \otimes Z)\Delta g_m\right\}, \\ -\Delta g_m^H (I \otimes Z)\Delta g_m + \sigma_m^{2(1-N_E)}\zeta_m - \sigma_{E,m}^2 \le 0. \end{cases} \tag{17}$$

Nextly, we introduce the following lemma to handle the channel uncertainty.

Lemma 2 [23]. *Define the function*

$$f_j(x) = x^H A_j x + 2\Re\left\{b_j^H x\right\} + c_j, j = 1, 2, \tag{18}$$

where $\mathbf{A}_j = \mathbf{A}_j^H \in \mathbb{C}^{n\times n}$, $\mathbf{b}_j \in \mathbb{C}^{n\times 1}$, *and* $c_j \in \mathbb{R}$. *The implication* $f_1(x) \le 0 \Longrightarrow f_2(x) \le 0$ *holds if and only if there exists* $\lambda \ge 0$ *such that*

$$\lambda \begin{bmatrix} A_1 & b_1 \\ b_1^H & c_1 \end{bmatrix} - \begin{bmatrix} A_2 & b_2 \\ b_2^H & c_2 \end{bmatrix} \succcurlyeq 0, \tag{19}$$

provided that there exists a point x_0 *such that* $f_1(x_0) < 0$.

By using Lemma 2 with respect to Δg_m, (17) can be transformed to the following linear matrix inequality (LMI):

$$\begin{bmatrix} \varsigma_m \mathbf{I} + \mathbf{I} \otimes \mathbf{Z} & (\mathbf{I} \otimes \mathbf{Z})\bar{\mathbf{g}}_m \\ \bar{\mathbf{g}}_m^H (\mathbf{I} \otimes \mathbf{Z}) & -\varsigma_m \epsilon_m^2 + \bar{\mathbf{g}}_m^H (\mathbf{I} \otimes \mathbf{Z})\bar{g}_m - \sigma_{E,m}^{2(1-N_E)}\zeta_m + \sigma_{E,m}^2 \end{bmatrix} \succcurlyeq 0, \tag{20}$$

where $\varsigma_m \ge 0$ is the auxiliary variable.

Following a similar way, (15b) can be transformed as

$$\begin{bmatrix} \upsilon_m \mathbf{I} - \mathbf{\Psi}_m & -\mathbf{\Psi}_m \bar{g}_m \\ -\bar{\mathbf{g}}_m^H \mathbf{\Psi}_m^H & -\upsilon_m \delta_m^2 - \ln|\mathbf{B}_m| + \theta_m - \bar{\mathbf{g}}_m^H \mathbf{\Psi}_m \bar{\mathbf{g}}_m \end{bmatrix} \succcurlyeq 0, \tag{21}$$

where $\mathbf{\Psi}_m = (\mathbf{B}_m^{-1})^T \otimes (\mathbf{Q} - \tilde{\mathbf{Q}} + \mathbf{Z} - \tilde{\mathbf{Z}})$ and $\upsilon_m \ge 0$ is the auxiliary variable.

Besides, the ER's harvested energy constraint (11e) can be turned into

$$\begin{bmatrix} \lambda_m \mathbf{I} + (\mathbf{I} \otimes (\mathbf{Q} + \mathbf{Z})) & (\mathbf{I} \otimes (\mathbf{Q} + \mathbf{Z}))^H \bar{g}_m \\ \bar{\mathbf{g}}_m^H (\mathbf{I} \otimes (\mathbf{Q} + \mathbf{Z})) & -\lambda_m \delta_m^2 - \frac{E_{m,th}}{\eta_m} + N_E \sigma_{E,m}^2 + \bar{\mathbf{g}}_m^H (\mathbf{I} \otimes (\mathbf{Q} + \mathbf{Z}))\bar{\mathbf{g}}_m \end{bmatrix} \succcurlyeq 0, \tag{22}$$

where $\lambda_m \ge 0$ is the auxiliary variable.

By combining these steps, we obtain the following problem:

$$\mathrm{P4}: \max_{\mathbf{Q},\mathbf{Z},t,\gamma_1,\gamma_2,\zeta_m,\theta_m,\varsigma_m,\upsilon_m,\lambda_m} \frac{\gamma_1 - \gamma_2}{\mu\mathrm{Tr}(\mathbf{Q} + \mathbf{Z}) + P_c}, \tag{23a}$$

$$\text{s.t.} (11\text{c}) - (11\text{e}), (11\text{h}), (18) - (20), \tag{23b}$$

$$\zeta_m \ge 0, \theta_m \ge 0, \varsigma_m \ge 0, \upsilon_m \ge 0, \lambda_m \ge 0. \tag{23c}$$

The remaining task is to handle the fractional objective (23a). Different from the commonly used Dinkelbach method, which turns the fractional objective into a subtractive form, we will change (23a) into exponential functions. Then, the monotonicity of exponential functions will be utilized to simplify the objective [24]. Specifically, via introducing slack variables x_1 and x_2, (23) can be turned into

$$\mathrm{P5}: \max_{\Omega} x_1 - x_2, \tag{24a}$$

$$\text{s.t.} (21\text{b}), (21\text{c}), \tag{24b}$$

$$\gamma_1 - \gamma_2 \ge e^{x_1}, \tag{24c}$$

$$\mu\mathrm{Tr}(\mathbf{Q} + \mathbf{Z}) + P_c \le e^{x_2}, \tag{24d}$$

where $\mathbf{\Omega} \triangleq \{\mathbf{Q}, \mathbf{Z}, t, \gamma_1, \gamma_2, \zeta_m, \theta_m, \varsigma_m, \upsilon_m, \lambda_m, x_1, x_2\}$ denotes the set of all optimization variables.

The only nonconvex part in (24) is (24d). Via the first-order Taylor expansion, around given point $\tilde{x}_2$, (24d) can be approximated as

$$\mu\mathrm{Tr}(\mathbf{Q} + \mathbf{Z}) + P_c \le e^{\tilde{x}_2}(x_2 - \tilde{x}_2 + 1). \tag{25}$$

To this end, we turn (10) into the following problem:

$$\mathrm{P6}: \max_{\Omega} x_1 - x_2, \tag{26a}$$

$$\text{s.t.} (22\text{b}), (22\text{c}), (23). \tag{26b}$$

Then, the remaining task is to handle the rank relaxation introduced by Lemma 1. In the following, we will propose a penalty-based method. Firstly, by invoking Lemma 1, we have

$$\begin{aligned} \mathrm{rank}\left(\mathbf{G}_m^H \mathbf{Z} \mathbf{G}_m\right) = 1 &\Longleftrightarrow \left|\mathbf{I} + \mathbf{G}_m^H \mathbf{Z} \mathbf{G}_m\right| \\ &\le 1 + \mathrm{Tr}\left(\mathbf{G}_m^H \mathbf{Z} \mathbf{G}_m\right) \Longleftrightarrow \ln\left|\mathbf{I} + \mathbf{G}_m^H \mathbf{Z} \mathbf{G}_m\right| \\ &\le \ln\left(1 + \mathrm{Tr}\left(\mathbf{G}_m^H \mathbf{Z} \mathbf{G}_m\right)\right). \end{aligned} \tag{27}$$

$\ln|\mathbf{I} + \mathbf{G}_m^H \mathbf{Z} \mathbf{G}_m|$ is a concave function w.r.t $\mathbf{Z}$. To handle the concavity, the penalty-based method is utilized by putting the constraint into the objective function. Then, (26) can be recast as

$$\max_{\Omega, z_m} x_1 - x_2 + k\sum_{m=1}^{M}\left[\ln(z_m) - \ln\left|\mathbf{I} + G_m^H \mathbf{Z} \mathbf{G}_m\right|\right], \tag{28a}$$

$$\text{s.t.} (22\text{b}), (22\text{c}), (23), \tag{28b}$$

$$z_m \le 1 + \mathrm{Tr}\left(\mathbf{G}_m^H \mathbf{Z} \mathbf{G}_m\right), \tag{28c}$$

where κ is a penalty factor penalizing the violation of constraint $\mathrm{rank}\,(\mathbf{G}_m^H \mathbf{Z} \mathbf{G}_m) = 1$. In addition, the upper bound of $\ln|I + G_m^H Z G_m|$ can be obtained by using the first-order

[1] **Initialization:** $i = 1$, set P_s, $E_{R,th}$, $E_{m,th}$, R_{th}.
[2] **repeat**
a) Obtain $\{\mathbf{Q}^{(i)}, \mathbf{Z}^{(i)}, t^{(i)}\}$ and $SEE^{(i)}$ with fixed $\{\tilde{\mathbf{Q}}, \tilde{\mathbf{Z}}, \tilde{t}\}$ via solving (30).
b) Update $\{\tilde{Q}, \tilde{Z}, \tilde{t}\} = \{Q^{(i)}, Z^{(i)}, t^{(i)}\}$.
c) $i = i + 1$.
[3] **until** $SEE^{(i)} - SEE^{(i-1)} < \kappa$.
[4] **Output** $\{\mathbf{W}^{\star}, \mathbf{Z}^{\star}, t^{\star}\}$ and $SEE^{\star}$.

Algorithm 1: Iterative algorithm for (30).

Taylor approximation as

$$\ln\left|\mathbf{I}+\mathbf{G}_m^H\mathbf{Z}\mathbf{G}_m\right| \le \ln\left|\mathbf{I}+\mathbf{G}_m^H\mathbf{Z}^{(i)}\mathbf{G}_m\right| + \mathrm{Tr}\cdot\left(\left(\mathbf{I}+\mathbf{G}_m^H\mathbf{Z}^{(i)}\mathbf{G}_m\right)^{-1}\left(\mathbf{Z}-\mathbf{Z}^{(i)}\right)\right). \tag{29}$$

Based on (29), (28) can be approximated as

$$\max_{\Omega,z_m} x_1 - x_2 + k\sum_{m=1}^{M}\ln(z_m) - k\sum_{m=1}^{M}\mathrm{Tr}\left(\left(I+G_m^H Z^{(i)} G_m\right)^{-1}\left(Z-Z^{(i)}\right)\right), \tag{30a}$$

$$\text{s.t.}(22\text{b}), (22\text{c}), (23), (26\text{c}). \tag{30b}$$

(30) is convex w.r.t $\mathbf{Z}$, which can be efficiently solved by the convex programming toolbox CVX [25]. The entail iterative algorithm for (30) is summarized in Algorithm 1, in which $\{\mathbf{Q}^{(i)}, \mathbf{Z}^{(i)}, t^{(i)}\}$ is the obtained optimal solution in the i-th iteration, respectively. In addition, $\mathrm{SEE}^{(i)}$ is the optimal value of (30) in the i-th iteration; κ denotes the stopping criterion, namely, the tolerance [h].

Here, we analyze the computational complexity of the proposed method. Since (26) involves the LMI constraints and the second-order cone (SOC) constraints, we can estimate the complexity based on the framework in [26]. Specifically, the complexity for a κ-optimal solution to (26) is on the order of $\ln(1/\kappa)\sqrt{\varpi}\vartheta$, where $\varpi = 6N_TN_E + 2N_T + 15$, $\vartheta = 6n(N_TN_E+1)^3 + 36n^2(N_TN_E+1)^2 + 2nN_T^3 + 4n^2N_T^2$, and $n = \mathcal{O}(2N_T^2)$, respectively. On the other hand, when the Dinkelbach algorithm is used, the computational complexity is $\tau\ln(1/\kappa)\sqrt{\varpi}\vartheta$, where τ denoted the numbers of one-dimensional search, $\varpi = 6N_TN_E + 2N_T + 12$, $\vartheta = 6n(N_TN_E+1)^3 + 36n^2(N_TN_E+1)^2 + 2nN_T^3 + 4n^2N_T^2$, and $n = \mathcal{O}(2N_T^2)$, respectively. From this comparison, we can conclude that the proposed method can achieve lower complexity than the Dinkelbach algorithm, mainly due to the fact that the proposed method does not conduct the one-dimensional search procedure.

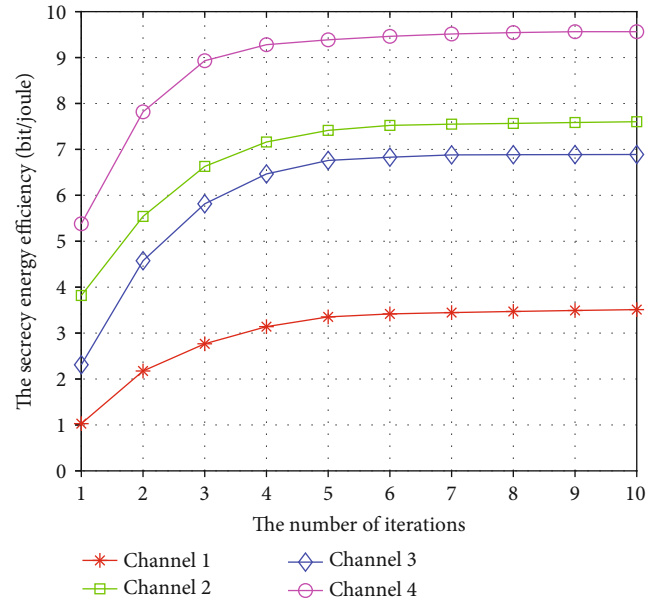

Figure 2: Convergence behaviour of the proposed method.

4. Simulation Results

In this section, we provide some numerical results to testify the availability of our proposed scheme. Unless specified, the simulation setting is assumed as follows: $N_T = d = 4$, $N_D = 2$, $N_E = 2$, $M = 2$, $P_s = 10$dBW, $P_c = 0$dBW, $\mu = 1$, $R_{th} = 2$bit/s/Hz, $E_{R,th} = E_{m,th} = -50$dBW, $\forall m$, $\sigma_D^2 = \sigma_P^2 = \sigma_{E,m}^2 = -80$dBW, and $\alpha = \eta_m = 1, \forall m$. In addition, each entry of $\mathbf{H}$ and $\bar{\mathbf{G}}_m$ is randomly generated by $\mathcal{CN}(0, 10^{-3})$, and the channel uncertainties are $\varepsilon_m = 10^{-6}, \forall m$. In addition, we also compare our design with several other methods: (1) the proposed method in the case of perfect CSI, which can be seen as the benchmark of the robust design; (2) the no AN design, e.g., setting $\mathbf{Z} = 0$ while only optimizing $\mathbf{W}$ and ρ; (3) the fixed PS ratio design, e.g., setting PS ratio $\rho = 0.5$ while only optimizing $\mathbf{W}$ and $\mathbf{Z}$; (4) the nonlinear EH model, e.g., the relationship between the input power E_{in} and output power E_{out} of the EH circuit is modeled as $E_{\text{out}} = ((M/(1+e^{(-a(E_{\text{in}}-b))})) - M\Omega)/(1-\Omega)$, where M is a constant denoting the maximum harvested power at the receiver when the EH circuit is saturated, a reflects the nonlinear charging rate with

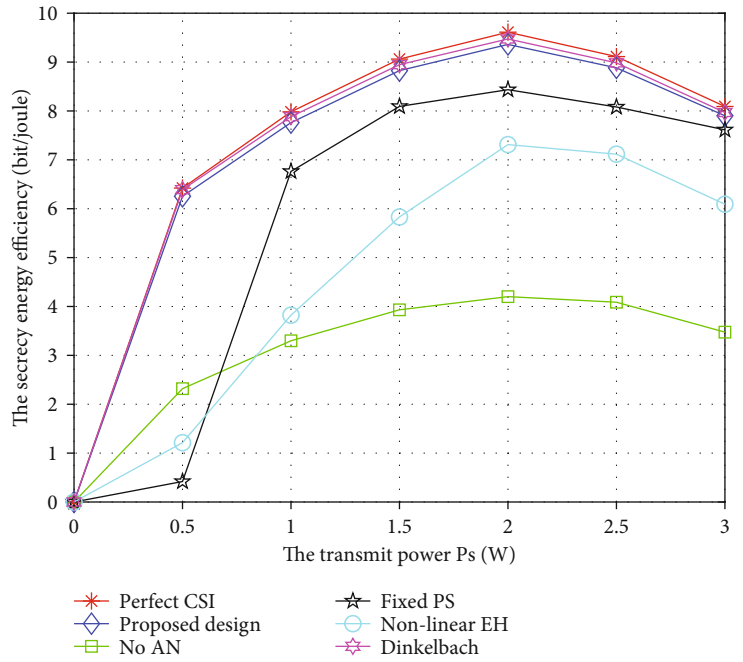

Figure 3: SEE versus the transmit power.

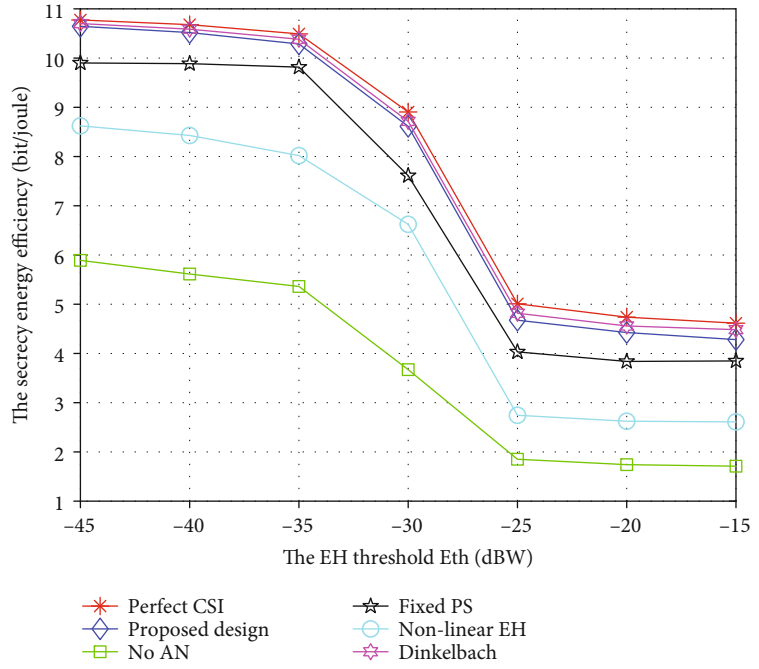

Figure 4: SEE versus the secrecy rate threshold.

respect to the input power, b is related to the minimum turn-on voltage of an EH circuit, and $\Omega = 1/(1 + e^{ab})$, where we set $M = 20$mW, $a = 6400$, and $b = 0.003$ [13]; and (5) the Dinkelbach method. These methods are labeled as "proposed design," "perfect CSI," "no AN," "fixed PS," "nonlinear EH," and "Dinkelbach," respectively.

Firstly, we investigate the convergency of the proposed design. Figure 2 shows several examples of the convergence behavior with random channel realizations. From this figure, we can see that the proposed method can always converge to the optimal solution within limited iterative numbers.

Nextly, Figure 3 plots the SEE versus the transmit power P_s. From Figure 3, we can see that the efficiency firstly increases and then decreases with P_s for all these methods while the proposed design outperforms the other designs; this is because when P_s is relatively small compared to P_c,

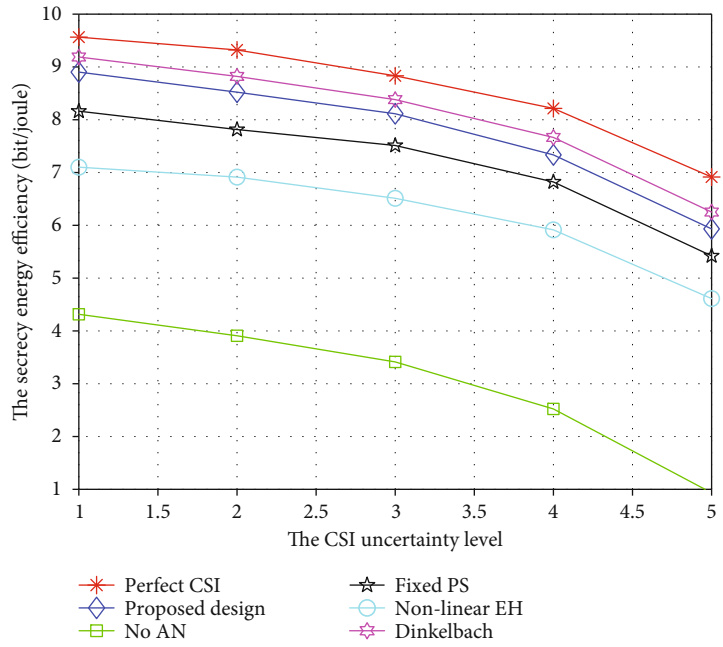

Figure 5: SEE versus the CSI uncertainty level.

the SEE metric is mainly determined by the information rate in the numerator. By contrast, when P_s becomes large, the SEE metric is also determined by the transmit power in the denominator. As a result, the SEE reaches a saturated point. In addition, the proposed method can obtain better performance than several other benchmarks, and the performance gap between the proposed method and the Dinkelbach method is negligible. Besides, the linear EH model can achieve higher SEE than the nonlinear EH model, which is mainly due to that more output power can be obtained for the linear EH circuit when given the same input power.

Then, Figure 4 shows the SEE versus the harvested power threshold E_{th}. From Figure 4, we find that with the increase in E_{th}, the SEE decreases for all the methods. However, the proposed design always achieves a higher efficiency than the other designs. While the no AN method suffers obvious performance loss. This is mainly due to AN's dual role: AN is able to degrade Eve's reception and act as ER's energy source at the same time, which compensates for the loss of secrecy incurred by the SWIPT scheme. Besides, dynamic PS is beneficial to coordinate ID and EH; thus, higher SEE can be obtained than the fixed PS scheme.

Lastly, Figure 5 shows the SEE versus the CSI uncertainty level ε_m. From Figure 5, we find that with the increase in ε_m, the SEE decreases for all the methods. Since with the increase in ε_m, the robust secrecy rate tends to decrease in the condition of the same transmit power, the SEE decreases. This result suggests that the CSI uncertainty level has a huge impact on the SEE performance.

5. Conclusion

In this work, we have investigated the secrecy design in the MIMO SWIPT channel. Specifically, we formulated the SEE problem by jointly optimizing the precoding matrix, the AN covariance, and the PS ratio with multiple constraints. We utilized the SCA and penalty method to solve the formulated highly nonconvex problem. Simulation results validated that significant SEE improvement can be obtained with the proposed method.

Data Availability

The data used to support the findings of this study are available from the corresponding author upon request.

Conflicts of Interest

The authors declare that they have no known competing financial interests or personal relationships that could have appeared to influence the work reported in this paper.

Acknowledgments

This work was supported by the National Natural Science Foundation of China (Nos. 61771486 and 62001515) and Jiangsu Planned Projects for Postdoctoral Research Funds (No. 2019K090).

References

[1] S. Zhang, Q. Wu, S. Xu, and G. Y. Li, "Fundamental green tradeoffs: progresses, challenges, and impacts on 5G networks," *IEEE Communications Surveys & Tutorials*, vol. 19, no. 1, pp. 33–56, 2017.

[2] T. D. Ponnimbaduge Perera, D. N. K. Jayakody, S. K. Sharma, S. Chatzinotas, and J. Li, "Simultaneous wireless information and power transfer (SWIPT): recent advances and future challenges," *IEEE Communications Surveys & Tutorials*, vol. 20, no. 1, pp. 264–302, 2018.

[3] A. Zappone, E. Bjornson, L. Sanguinetti, and E. Jorswieck, "Globally optimal energy-efficient power control and receiver design in wireless networks," *IEEE Transactions on Signal Processing*, vol. 65, no. 11, pp. 2844–2859, 2017.

[4] K. Xiong, B. Wang, and K. J. R. Liu, "Rate-energy region of SWIPT for MIMO broadcasting under nonlinear energy harvesting model," *IEEE Transactions on Wireless Communications*, vol. 16, no. 8, pp. 5147–5161, 2017.

[5] F. Heliot and R. Tafazolli, "Optimal energy-efficient source and relay precoder design for cooperative MIMO-AF systems," *IEEE Transactions on Signal Processing*, vol. 66, no. 3, pp. 573–588, 2018.

[6] Y. Liu, H.-H. Chen, and L. Wang, "Physical layer security for next generation wireless networks: theories, technologies, and challenges," *IEEE Communications Surveys & Tutorials*, vol. 19, no. 1, pp. 347–376, 2017.

[7] Y. Wu, A. Khisti, C. Xiao, G. Caire, K. K. Wong, and X. Gao, "A survey of physical layer security techniques for 5G wireless networks and challenges ahead," *IEEE Journal on Selected Areas in Communications*, vol. 36, no. 4, pp. 679–695, 2018.

[8] D. Wang, B. Bai, W. Zhao, and Z. Han, "A survey of optimization approaches for wireless physical layer security," *IEEE Communications Surveys & Tutorials*, vol. 21, no. 2, pp. 1878–1911, 2019.

[9] W. Mei, Z. Chen, and J. Fang, "Artificial noise aided energy efficiency optimization in MIMOME system with SWIPT," *IEEE Communications Letters*, vol. 21, no. 8, pp. 1795–1798, 2017.

[10] A. Nasir, H. Tuan, T. Duong, and H. V. Poor, "Secure and energy-efficient beamforming for simultaneous information and energy transfer," *IEEE Transactions on Wireless Communications*, vol. 16, no. 11, pp. 7523–7537, 2017.

[11] Z. Chu, H. Xing, M. Johnston, and S. le Goff, "Secrecy rate optimizations for a MISO secrecy channel with multiple multi-antenna eavesdroppers," *IEEE Transactions on Wireless Communications*, vol. 15, no. 1, pp. 283–297, 2016.

[12] Z. Chu, Z. Zhu, M. Johnston, and S. Y. le Goff, "Simultaneous wireless information power transfer for MISO secrecy channel," *IEEE Transactions on Vehicular Technology*, vol. 65, no. 9, pp. 6913–6925, 2016.

[13] H. Niu, D. Guo, Y. Huang, and B. Zhang, "Robust energy efficiency optimization for secure MIMO SWIPT systems with non-linear EH model," *IEEE Communications Letters*, vol. 21, no. 12, pp. 2610–2613, 2017.

[14] Z. Zhu, Z. Chu, F. Zhou, H. Niu, Z. Wang, and I. Lee, "Secure beamforming designs for secrecy MIMO SWIPT systems," *IEEE Wireless Communications Letters*, vol. 7, no. 3, pp. 424–427, 2018.

[15] Y. Yuan and Z. Ding, "Outage constrained secrecy rate maximization design with SWIPT in MIMO-CR systems," *IEEE Transactions on Vehicular Technology*, vol. 67, no. 6, pp. 5475–5480, 2018.

[16] L. Ni, X. Da, H. Hu, M. Zhang, and K. Cumanan, "Outage constrained robust secrecy energy efficiency maximization for EH cognitive radio networks," *IEEE Wireless Communications Letters*, vol. 21, no. 12, pp. 2610–2613, 2020.

[17] H. Sun, F. Zhou, R. Q. Hu, and L. Hanzo, "Robust beamforming design in a NOMA cognitive radio network relying on SWIPT," *IEEE Journal on Selected Areas in Communications*, vol. 37, no. 1, pp. 142–155, 2019.

[18] F. Zhou and R. Q. Hu, "Computation efficiency maximization in wireless-powered mobile edge computing networks," *IEEE Transactions on Wireless Communications*, vol. 19, no. 5, pp. 3170–3184, 2020.

[19] F. Zhou, Z. Chu, H. Sun, R. Q. Hu, and L. Hanzo, "Artificial noise aided secure cognitive beamforming for cooperative MISO-NOMA using SWIPT," *IEEE Journal on Selected Areas in Communications*, vol. 36, no. 4, pp. 918–931, 2018.

[20] Y. Lu, K. Xiong, P. Fan, Z. Ding, Z. Zhong, and K. B. Letaief, "Global energy efficiency in secure MISO SWIPT systems with non-linear power-splitting EH model," *IEEE Journal on Selected Areas in Communications*, vol. 37, no. 1, pp. 216–232, 2019.

[21] Y. Zhou, F. Zhou, H. Zhou, D. W. K. Ng, and R. Q. Hu, "Robust trajectory and transmit power optimization for secure UAV-enabled cognitive radio networks," *IEEE Transactions on Communications*, vol. 68, no. 7, pp. 4022–4034, 2020.

[22] W. Dinkelbach, "On nonlinear fractional programming," *Management Science*, vol. 13, no. 7, pp. 492–498, 1967.

[23] Z.-Q. Luo, J. F. Sturm, and S. Zhang, "Multivariate nonnegative quadratic mappings," *SIAM Journal on Optimization*, vol. 14, no. 4, pp. 1140–1162, 2004.

[24] S. Boyd and L. Vandenberghe, *Convex Optimization*, Cambridge Univ. Press, Cambridge, U.K., 2004.

[25] M. Grant and S. Boyd, "CVX: Matlab software for disciplined convex programming, version 2.0 beta," 2012, http://cvxr.com/cvx.

[26] K. Wang, A. M.-C. So, T.-H. Chang, W.-K. Ma, and C.-Y. Chi, "Outage constrained robust transmit optimization for multi-user MISO downlinks: tractable approximations by conic optimization," *IEEE Transactions on Signal Processing*, vol. 62, no. 21, pp. 5690–5705, 2014.